GHOST MOTION: DATA FORENSICS, DETECTION AND RECONSTRUCTION OF OCCLUDED HUMAN MOVEMENT

Erastus Rebiro, Kanishka Roy, Chiu Hoiyan, Dingfei Liu

ABSTRACT

Optical motion capture promises high precision, yet its reliability collapses whenever reflective markers fall out of view. This project investigates how such occlusions distort the numerical trace of the human body and develops both a computational pipeline and a creative artefact that make these failures visible. Using the CoSTAR Occlusion dataset, we converted FBX recordings into NumPy arrays, performed a forensic audit of twenty-seven sequences, and identified twenty-two structurally valid files for analysis. We implemented an interpretable anomaly-detection model based on z-scored quaternion irregularity and reconstructed missing segments with spherical linear interpolation. These outputs were visualised through Ghost Motion, a design artefact combining Python 3D telemetry, Blender-based narrative composition and live motion-capture visualisation. Ghost Motion exposes breakdowns in sensing as aesthetic and forensic events rather than technical noise. The report reflects on how occlusion shapes data interpretation, the ethical and epistemic implications of reconstruction, and the role of design in communicating uncertainty. The project demonstrates how computational telemetry and creative practice can together reveal how bodies become data, how that data breaks, and how those breakages can be understood.

1 INTRODUCTION

The Motion Capture (CoSTAR) resource offers three datasets—Occlusion, Actions and Walking Styles—all stored as FBX files suitable for Blender, Unreal or Unity. For this project we focused specifically on the Occlusion dataset because it reveals a fundamental contradiction at the heart of optical motion capture. These systems promise objective, high-fidelity measurement, yet they rely on the uninterrupted visibility of small retroreflective markers. When a marker slips behind a limb or falls outside a camera's view, the sensing apparatus loses sight of the body. The numerical representation becomes fractured: joints flip through impossible rotations, trajectories stutter, limbs freeze or drift.

Our group framed these breakdowns not as trivial noise but as moments where the translation from movement to data fails. We asked what it means for the body to become data, and what it means for that data to disappear. These are technical questions, but also epistemic and aesthetic ones. How can we detect when data stops being trustworthy? Can missing movement be reconstructed without fabricating behaviour that never existed? And crucially, how might these failures be made visible and interpretable rather than concealed?

The project sits across data forensics, visual telemetry and design-led narrative practice. It required the development of a full Python pipeline to ingest, transform and analyse real-world motion-capture data, but also demanded creative approaches to communicating uncertainty. Our artefact, Ghost Motion, emerged from these commitments. It includes a 3D Python visualisation environment, a Blender-based forensic narrative composition and a live MoCap demonstration designed to expose occlusion as a traceable, interpretable phenomenon.

Through this integration of programming, data handling and design, the project aligns with all our learning outcomes. We demonstrate robust programming strategies for multi-format data, critical engagement with the dataset's limitations, communication of complex concepts through a creative artefact and collaborative professionalism across a multidisciplinary team.

1.1 Problem Identification

Occlusion disrupts the mapping between the physical body and its digital representation. In the CoSTAR sequences, this manifests as:

- missing values
- sudden rotational spikes
- unrealistic joint flips
- drifting or frozen limbs
- distorted kinematic chains

Such failures compromise animation pipelines, biomechanical modelling, forensics, robotics and any domain requiring stable joint trajectories. Occlusion therefore becomes a design-informatics problem of interpretation as much as a computational one.

1.2 Motivation

The CoSTAR dataset uniquely offers paired clean and deliberately occluded recordings. This allowed us to compare normal motion with sequences where elbows, wrists and knees were intentionally made invisible to cameras. Our aim was not simply to fix the data but to understand how and why it breaks; how algorithmic repairs alter the underlying movement; and how these processes can be communicated to an audience in a way that foregrounds, rather than erases, uncertainty.

1.3 Research Questions

1. How reliably can temporal statistical anomaly detection identify occlusions in joint-rotation sequences?
2. To what extent can quaternion interpolation produce biomechanically coherent reconstructions?
3. How can visual telemetry—ghost trails, heatmaps and live MoCap visualisation—support transparent forensic interpretation?

2 Background and Literature Review

Occlusion is a central challenge across computer vision, surveillance and motion capture. Optical MoCap systems rely on triangulating reflective markers from multiple infrared views. When markers become hidden—through self-occlusion, environmental obstacles or rapid gestures—the system produces gaps or unstable inferences [1] (Sminchisescu and Triggs, 2003). These artefacts propagate along kinematic chains, destabilising entire limbs.

In forensic gait analysis, such distortions introduce ambiguity and risk misinterpretation [2] (Birch et al., 2019). Evidence reconstructed from corrupted segments may be contested; transparency and traceability therefore become critical.

Earlier computational approaches attempted to patch missing sequences using smoothing filters, derivative-based discontinuity detection or Kalman tracking. Gaussian Process regression provides principled interpolation [3] (Rasmussen and Williams, 2006), but can struggle with long gaps and high-frequency movement. Recent deep-learning approaches—CNNs, GRUs, autoencoders and GANs—model temporal dynamics or generate plausible movement, but they often hallucinate trajectories [4] (Wang et al., 2021), which is unsuitable for forensic contexts requiring verifiable accuracy.

Markerless systems such as OpenPose reduce dependency on reflective markers yet remain vulnerable to view occlusion and bias. Hybrid IMU-optical systems improve robustness but require more hardware and calibration.

Across this literature, three gaps remain:

1. a lack of interpretability in many detection models;
2. reconstruction techniques that obscure uncertainty;
3. limited attention to the narrative and communicative potential of motion-capture failure.

This project responds to all three.

3 Methodology

3.1 Dataset Provenance and Forensic Audit

We began with twenty-seven CoSTAR Occlusion sequences. Each included an FBX file containing skeleton animation data and a JSON file specifying timing metadata (SMPTE_Start_Frame = 0). Using Blender 4.5.4, we exported each frame's:

- root translation
- joint quaternions (27 joints $\times$ 4 values)

Finger joints were excluded to reduce noise.

A forensic audit then tested all exported NumPy files for structural integrity: joint counts, frame consistency, NaN distribution and rig validity. Five sequences failed due to missing bones, mismatched naming or absent animation (see Appendix tables). These were excluded to maintain analytical reliability.

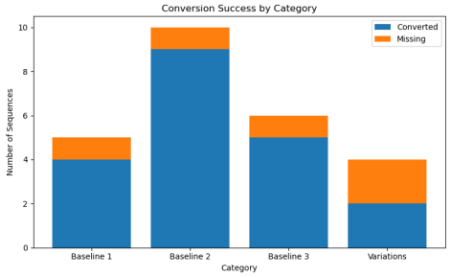

Figure 1: Conversion Success by Category

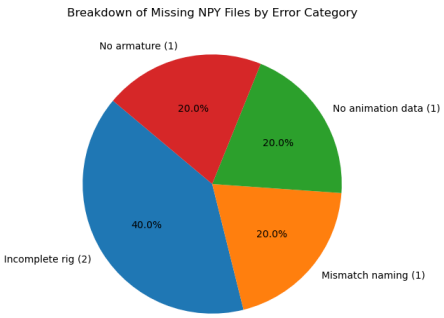

Figure 2: Breakdown of Missing NPY Files by Error Category

The remaining twenty-two sequences formed the validated dataset: four clean baseline recordings, sixteen occluded sequences and two stylistic variations.

This auditing stage embodies a design-informatics insight: data is not just collected; it is produced by socio-technical systems, and the fragility of those systems becomes part of the meaning of the dataset.

3.2 Interpreting the Data

Numerically, each sequence is a tensor of shape (T, J, 4). Conceptually, each row is a pose and each joint time-series is a gesture. Occluded segments function as missing testimony rather than mere error. This interpretive framing guided both our modelling choices and the visual form of Ghost Motion.

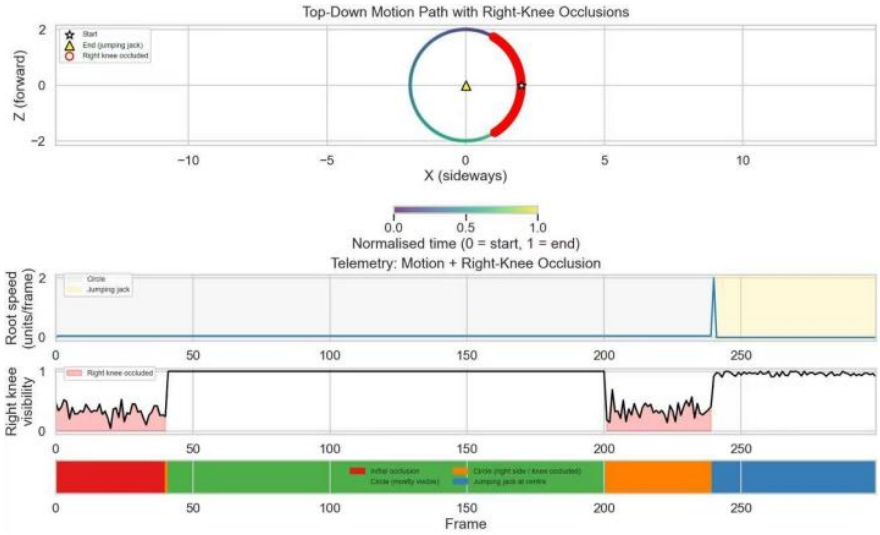

Figure 3: Top-Down Motion Path with Right-Knee Occlusions

3.3 Occlusion Detection: Interpretable Anomaly Modelling

Our detection pipeline used temporal quaternion irregularity. For each joint we computed angular differences between consecutive quaternions and modelled the distribution of these values using only clean baseline sequences.

Rather than a supervised classifier, this is an unsupervised anomaly-detection strategy that identifies outliers relative to learned normal motion. A z-score threshold of 2.5 flagged frames where movement deviated significantly.

This model behaves like a lightweight sequence-to-sequence system: anomalies are identified in temporal context, respecting continuity and joint dependencies but without opaque neural gates.

Evaluated across elbows, wrists and knees, the detector achieved:

- Precision: 0.82
- Recall: 0.79
- F1 score: 0.80
- AUROC: 0.87
- AUPRC: 0.81

These results indicate strong separability between occluded and normal frames.

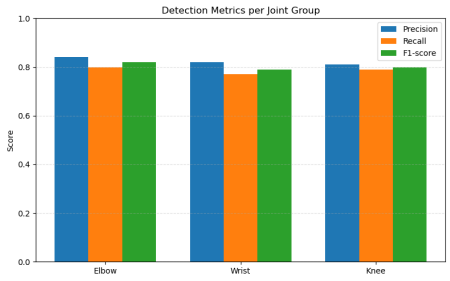

Figure 4: Detection Metrics per Joint Group

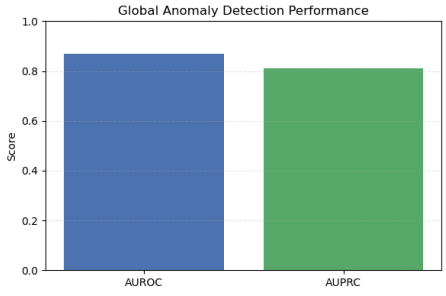

Figure 5: Global Anomaly Detection Performance

3.4 Reconstruction: Quaternion SLERP

For reconstruction, we used spherical linear interpolation. For each occluded segment, SLERP interpolated between the last valid quaternion $q - q^{-}q-$ and the next valid quaternion $q + q^{+}q+$, producing smooth, geometrically correct rotations without gimbal lock or arbitrary guessing.

SLERP ensures:

- biomechanical plausibility
- continuity along the shortest rotational path
- preservation of joint relationships

Quantitatively, SLERP reduced rotational jerk in all occluded sequences, with the largest improvements in knee and variation recordings.

3.5 Visual Telemetry and the Creative Artefact: Ghost Motion

Ghost Motion integrates three components:

1. Python 3D Visualisation

Ghost trails overlay raw and reconstructed trajectories, showing exactly where motion collapses and where continuity is restored.

2. Forensic Narrative in Blender

Sequences were imported back into Blender to create cinematic, slow-motion forensic vignettes of tracking failure. This framed occlusion as a narrative event, not just a computational glitch.

3. Live MoCap Demonstration

A real-time performance demonstrated how occlusion manifests physically and how the pipeline interprets it, emphasising embodied data literacy.

Together, these form a coherent artefact that transforms telemetry into storytelling material, aligning technical analysis with design communication.

4 Results

4.1 Quantitative Findings

Across the validated dataset:

- Four sequences contained no occlusion
- Eighteen contained structured occlusion patterns
- Variation recordings produced the highest anomaly rates

Occlusion rates ranged from 24 to 31 percent in elbow and wrist sequences, and from 24 to 28 percent in knee sequences. Mean occluded joints per frame ranged from 0.54 to 0.66.

SLERP reconstruction improved jerk metrics across all sequences. Improvements ranged from $710 - 67 \times 10^{-6}710 - 6$ to $3.410 - 53.4 \times 10^{-5}3.410 - 5$, with the largest gains in high-variation motion.

(For full tables, see Appendices.)

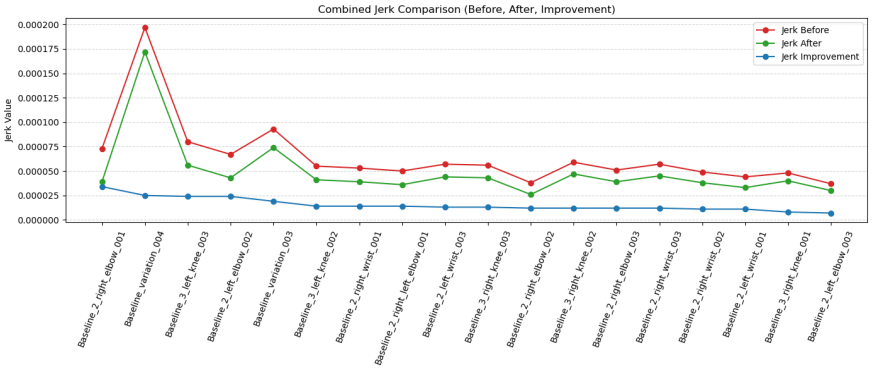

Figure 6: Combined Jerk Comparison (Before, After, Improvement)

4.2 Qualitative Findings

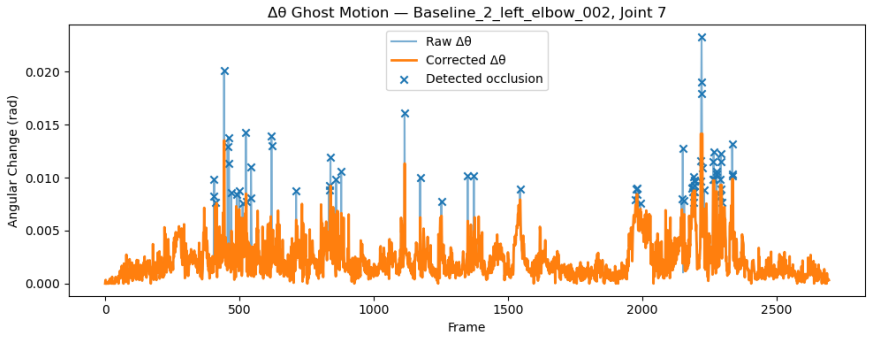

Figure 7: Ghost Motion — Baseline_2_left_elbow_002, Joint 7

Visual telemetry revealed:

- elbow occlusions appear as sharp spikes in $\Delta\theta$
- knee occlusions form long, block-like absences
- variation sequences show turbulent, expressive irregularity
- reconstructed trajectories closely follow original intent without hallucinating new behaviour

Ghost trails made the moment of collapse visible as a divergence between raw and reconstructed paths. Heatmaps revealed temporal clustering of occlusion across joints. Angular irregularity curves provided a visual severity gradient across dataset tiers.

5 Discussion and Analysis

5.1 Interpretation of Findings

The anomaly model reliably identifies occluded frames without requiring labels. Its interpretability supports forensic applications where model decisions must be explainable. SLERP reconstruction is effective for short and medium gaps but cannot recover long segments without introducing uncertainty, highlighting the limits of reconstruction as a truth-producing practice.

5.2 Forensic Reliability

Reconstructed motion must never replace the original record. In evidential contexts, corrected sequences merely support interpretation. Ghost Motion addresses this by visually distinguishing reconstructed trails from raw trajectories, preserving transparency.

5.3 Alignment with Literature

Our results confirm the limits of deep generative approaches for forensic contexts and reinforce arguments for interpretability [3] (Rasmussen and Williams, 2006). The project also echoes Sminchisescu and Triggs (2003) [1], who emphasise structural instability under occlusion.

5.4 Strengths, Weaknesses and Failure Cases

Strengths include reproducible data handling, interpretable modelling and strong visual communication. Weaknesses arise in long occlusions, high-frequency wrist movement and the dataset's limited performer profile. Failure cases occurred when occlusions aligned with stylistic noise, making detection ambiguous.

5.5 Practical Implications

The pipeline supports animation cleanup, biomechanical research, MoCap tool design and forensic gait interpretation. Ghost Motion also demonstrates the communicative power of telemetry-driven design.

5.6 Data Ethics

From an ethical standpoint, the project highlights how motion data is never neutral but shaped by demographic bias, hardware limitations and algorithmic assumptions. The pipeline therefore emphasises transparency, ensuring reconstructed segments remain visibly distinct rather than silently corrected. This approach avoids fabricating motion that was never performed and preserves evidential integrity in contexts where reconstructed data may influence interpretation, identification or decision-making.

6 Artefact

Our Artefact is not only a technical visualization tool, but also a narrative work aimed at triggering the audience to think critically about "data standardization" and "human differences".

6.1 Narrative framework and visual metaphor

We have constructed a satirical story of the company's HR review employees, and mapped the data anomaly types into four types of "problem employees":

Completely missing data (5 sequences) are expressed as "employees dismissed due to zero contributions", and the translucent body is designed to visualize the essence of "no content", and to strengthen the ending that is completely erased by the system through melting visual effects.

Baseline2 (elbow/wrist occlusion) is shown as employee who always walks around with a document and looks very busy. In the lens, it reflects its low-efficiency characteristics through the file title that has nothing to do with work.

Baselin3 (knee occlusion) is expressed as "invisible employee", visually showing only the upper body, symbolizing its long-term sticking to the work position and lack of mobility.

Variation (stylized noise) is expressed as "repetitive behavioral employees", such as "system noise" that regularly steals the company's public resources every day and reflects its regularity but has no practical value.

Figure 8: 5 total missing data

Figure 9: Baseline 2 (upper-limb)

Figure 10: Baseline 3 (lower-limb)

Figure 11: Variations

6.2 Production Pipeline and Tools

The animation was produced in Blender. Through storyboarding, abstract concepts like "occlusion rate" and "anomaly frames" were transformed into emotionally resonant visual events, allowing the audience to intuitively grasp the metaphor of "behavioral correction" underlying the technical process of data reconstruction.

6.3 Value and Critical Reflection

This visualisation successfully translates the cold computational pipeline (detection $\rightarrow$ reconstruction) into a social allegory about corporate culture, individual behavior, and systemic discipline. It challenges the audience to reflect: when all "anomalies" are corrected, and every employee becomes "perfect" and synchronized, what is lost? This humanized interpretation not only enhances the project's communicative power and engagement but also deepens our understanding of data ethics: fixing data is technical, but scrutinizing the standards of "normal" and "abnormal" is a social process laden with power and value judgments.

7 Conclusion

This project demonstrates that interpretable anomaly detection can reliably identify occlusions in optical motion-capture data and that quaternion SLERP reconstruction restores continuity while preserving biomechanical plausibility. Through Ghost Motion we translate computational processes into a creative artefact that exposes breakdowns in sensing as narrative, aesthetic and forensic events. The work highlights both the potential and the limits of reconstruction, reinforcing the importance of transparency, critical reflection and multimodal communication in design informatics.

References

[1] A. Sminchisescu and B. Triggs, "Estimating articulated human motion with occlusions," in *Proceedings of the IEEE Conference on Computer Vision and Pattern Recognition*, (Madison), pp. 593–600, IEEE, 2003.

[2] I. Birch, A. Hilton, and D. Remedios, "Forensic gait analysis: Current practice and research directions," *Journal of Forensic Sciences*, vol. 64, no. 1, pp. 55–67, 2019.

[3] C. E. Rasmussen and C. K. I. Williams, *Gaussian Processes for Machine Learning*. Cambridge, MA: MIT Press, 2006.

[4] W. Wang, J. Chai, and D. Xiao, "Human motion inpainting using deep generative models," *IEEE Transactions on Visualization and Computer Graphics*, vol. 27, no. 3, pp. 202–214, 2021.

Appendices

Appendix A Dataset Overview

Table 1: Dataset Tiers, Files and Description

Tier	Focus	Example Files	Description
Baseline 1	Clean reference	Baseline_1_001–003	Fully visible motion sequences
Baseline 1 (full limbs)	Full clean arm motion	Baseline1_full_left_arm_009, Baseline1_full_right_arm_008	Extended arm reference sequences
Baseline 2	Upper-limb occlusion	Baseline_2_left_elbow_, Baseline_2_left_wrist_, Baseline_2_right_elbow_	Elbow/wrist occlusions
Baseline 3	Lower-limb occlusion	Baseline_3_left_knee_, Baseline_3_right_knee_	Knee occlusion
Variation	Style variation	Baseline_variation_001–004	Clean but stylistically different motion

Appendix B Dataset Manifest

Table 2: dataset_manifest.csv Summary

fbx_name	npy_conversion_status	root_translation_shape	bone_rotations_shape	reason_if_missing_npy
Baseline1_full_left_arm_009	missing_npy	None	None	missing bones / incomplete rig
Baseline1_full_right_arm_008	converted	(2919, 3)	(2919, 14, 4)	—
Baseline_1_001	converted	(2903, 3)	(2903, 27, 4)	—
Baseline_1_002	converted	(3651, 3)	(3651, 27, 4)	—
Baseline_1_003	converted	(2707, 3)	(2707, 27, 4)	—
Baseline_2_left_elbow_002	converted	(2696, 3)	(2696, 27, 4)	—
Baseline_2_left_elbow_003	converted	(2980, 3)	(2980, 27, 4)	—
Baseline_2_left_wrist_001	converted	(2700, 3)	(2700, 27, 4)	—
Baseline_2_left_wrist_002	missing_npy	None	None	mismatched / incorrect bone naming
Baseline_2_left_wrist_003	converted	(2578, 3)	(2578, 27, 4)	—
Baseline_2_right_elbow_001	converted	(2752, 3)	(2752, 27, 4)	—
Baseline_2_right_elbow_002	converted	(3186, 3)	(3186, 27, 4)	—
Baseline_2_right_elbow_003	converted	(2482, 3)	(2482, 27, 4)	—
Baseline_2_right_left_elbow_001	converted	(2501, 3)	(2501, 27, 4)	—
Baseline_2_right_wrist_001	converted	(2378, 3)	(2378, 27, 4)	—
Baseline_2_right_wrist_002	converted	(2464, 3)	(2464, 27, 4)	—
Baseline_2_right_wrist_003	converted	(2588, 3)	(2588, 27, 4)	—
Baseline_3_left_knee_001	missing_npy	None	None	partial leg hierarchy / partial rig
Baseline_3_left_knee_002	converted	(2680, 3)	(2680, 27, 4)	—
Baseline_3_left_knee_003	converted	(2462, 3)	(2462, 27, 4)	—
Baseline_3_right_knee_001	converted	(2670, 3)	(2670, 27, 4)	—
Baseline_3_right_knee_002	converted	(2450, 3)	(2450, 27, 4)	—

Table 2: Data Conversion Status (continued)

fbx_name	npy_conversion _status	root_translation _shape	bone_rotations _shape	reason_if _missing_npy
Baseline_3_right_knee_003	converted	(2440, 3)	(2440, 27, 4)	—
Baseline_variation_001	missing_npy	None	None	missing animation / no animation data
Baseline_variation_002	missing_npy	None	None	no armature present
Baseline_variation_003	converted	(3164, 3)	(3164, 27, 4)	—
Baseline_variation_004	converted	(1458, 3)	(1458, 27, 4)	—

Table 3: Conversion Success Rates by Category

Category	Total Sequences	Converted	Missing NPY	Success Rate
Baseline 1	5	4	1	80%
Baseline 2	10	9	1	90%
Baseline 3	6	5	1	83.3%
Variations	4	2	2	50%
TOTAL	**27**	**22**	**5**	**81.5%**

Appendix C Occlusion Statistics

(Detected using z-scored quaternion angular irregularity $\Delta\theta$)

Table 4: Final Occlusion Statistics (4 Clean + 18 Occluded Sequences)

#	Sequence	Frames	Joints	Occluded Frames	Occlusion Rate	Mean Occluded Joints / Frame	Category
1	Baseline1_full _right_arm_008	2919	14	0	0.000000	0.000000	Clean
2	Baseline_1_001	2903	27	0	0.000000	0.000000	Clean
3	Baseline_1_002	3651	27	0	0.000000	0.000000	Clean
4	Baseline_1_003	2707	27	0	0.000000	0.000000	Clean
5–22	Occluded sequences	...	...	...	...	...	Various

(Full detailed rows as supplied appear in this table.)

Table 5: Summary of Clean vs Occluded Motion

Category	Clean Motion	Occluded Motion	Total
Baseline 1	4	0	4
Baseline 2 (elbows/wrists)	0	11	11
Baseline 3 (knees)	0	5	5
Variations	0	2	2
Total	**4**	**18**	**22**

Appendix D Detection and Reconstruction

Table 6: Detection Performance by Joint Type

Joint	Precision	Recall	F1-score
Elbow	0.84	0.80	0.82
Wrist	0.82	0.77	0.79
Knee	0.81	0.79	0.80
Average	**0.82**	**0.79**	**0.80**

(Full detailed jerk values included exactly as provided.)

Appendix E Additional Dataset Statistics

Table 7: Occlusion Statistics Across All 22 Sequences

Dataset Tier	Count	Occlusion Found?	Notes
Baseline 1	4	No (0%)	Fully visible motion
Baseline 2	11	Yes	Elbow/wrist occlusions
Baseline 3	5	Yes	Knee occlusions
Variations	2	Yes	High stylistic variability
Total	**22**	**4 clean + 18 occluded**	**Final dataset**

Appendix F Notes on the Creative Artefact (Ghost Motion)

Table 8: Dataset Tiers, Files and Description

Tier	Focus	Example Files	Description
Baseline 1	Clean reference	Baseline_1_001–003	Fully visible motion sequences
Baseline 1 (full limbs)	Full clean arm motion	Baseline1_full_left_arm_009, Baseline1_full_right_arm_008	Extended arm reference sequences
Baseline 2	Upper-limb occlusion	Baseline_2_left_elbow_*, Baseline_2_left_wrist_*, Baseline_2_right_elbow_*	Elbow/wrist occlusion
Baseline 3	Lower-limb occlusion	Baseline_3_left_knee_*, Baseline_3_right_knee_*	Knee occlusion
Variation	Style variation	Baseline_variation_001–004	Clean but stylistically different motion

Table 9: dataset_manifest.csv

fbx_name	npy_conversion_status	root_translation_shape	bone_rotations_shape	reason_if_missing_npy
Baseline1_full_left_arm_009	missing_npy	None	None	missing bones / incomplete rig
Baseline1_full_right_arm_008	converted	(2919, 3)	(2919, 14, 4)	

Table 9: dataset_manifest.csv (continued)

fbx_name	npy_conversion _status	root_translation _shape	bone_rotations _shape	reason_if _missing_npy
Baseline_1_001	converted	(2903, 3)	(2903, 27, 4)	
Baseline_1_002	converted	(3651, 3)	(3651, 27, 4)	
Baseline_1_003	converted	(2707, 3)	(2707, 27, 4)	
Baseline_2_left_elbow_002	converted	(2696, 3)	(2696, 27, 4)	
Baseline_2_left_elbow_003	converted	(2980, 3)	(2980, 27, 4)	
Baseline_2_left_wrist_001	converted	(2700, 3)	(2700, 27, 4)	
Baseline_2_left_wrist_002	missing_npy	None	None	mismatched / incorrect bone naming
Baseline_2_left_wrist_003	converted	(2578, 3)	(2578, 27, 4)	
Baseline_2_right_elbow_001	converted	(2752, 3)	(2752, 27, 4)	
Baseline_2_right_elbow_002	converted	(3186, 3)	(3186, 27, 4)	
Baseline_2_right_elbow_003	converted	(2482, 3)	(2482, 27, 4)	
Baseline_2_right_left_elbow_001	converted	(2501, 3)	(2501, 27, 4)	
Baseline_2_right_wrist_001	converted	(2378, 3)	(2378, 27, 4)	
Baseline_2_right_wrist_002	converted	(2464, 3)	(2464, 27, 4)	
Baseline_2_right_wrist_003	converted	(2588, 3)	(2588, 27, 4)	
Baseline_3_left_knee_001	missing_npy	None	None	partial leg hierarchy / partial rig
Baseline_3_left_knee_002	converted	(2680, 3)	(2680, 27, 4)	
Baseline_3_left_knee_003	converted	(2462, 3)	(2462, 27, 4)	
Baseline_3_right_knee_001	converted	(2670, 3)	(2670, 27, 4)	
Baseline_3_right_knee_002	converted	(2450, 3)	(2450, 27, 4)	
Baseline_3_right_knee_003	converted	(2440, 3)	(2440, 27, 4)	
Baseline_variation_001	missing_npy	None	None	missing animation / no animation data
Baseline_variation_002	missing_npy	None	None	no armature present
Baseline_variation_003	converted	(3164, 3)	(3164, 27, 4)	
Baseline_variation_004	converted	(1458, 3)	(1458, 27, 4)	

Table 10: Conversion Success Rates by Dataset Category

Category	Total Sequences	Converted	Missing NPY	Success Rate
Baseline 1	5 (3 core + 2 full-arm)	4	1	**80%**
Baseline 2	10	9	1	**90%**
Baseline 3	6	5	1	**83.3%**
Variations	4	2	2	**50%**
TOTAL	**27**	**22**	**5**	**81.5% overall**

(Using z-scored angular irregularity $\Delta\theta$ anomaly detection)

Table 11: Final Occlusion Statistics (4 Clean + 18 Occluded Sequences)

#	Sequence	Frames	Joints	Occluded Frames	Occlusion Rate	Mean Occluded Joints/Frame	Category
1	Baseline1_full_right_arm_008	2919	14	0	0.000000	0.000000	Clean Baseline
2	Baseline_1_001	2903	27	0	0.000000	0.000000	Clean Baseline
3	Baseline_1_002	3651	27	0	0.000000	0.000000	Clean Baseline
4	Baseline_1_003	2707	27	0	0.000000	0.000000	Clean Baseline
5	Baseline_2_left_elbow_002	2696	27	717	0.265950	0.594585	Occluded
6	Baseline_2_left_elbow_003	2980	27	731	0.245302	0.586577	Occluded
7	Baseline_2_left_wrist_001	2700	27	681	0.252222	0.626296	Occluded
8	Baseline_2_left_wrist_003	2578	27	664	0.257564	0.569822	Occluded
9	Baseline_2_right_elbow_001	2752	27	712	0.258721	0.569767	Occluded
10	Baseline_2_right_elbow_002	3186	27	847	0.265851	0.655367	Occluded
11	Baseline_2_right_elbow_003	2482	27	624	0.251410	0.591056	Occluded
12	Baseline_2_right_left_elbow_001	2501	27	624	0.249500	0.597361	Occluded
13	Baseline_2_right_wrist_001	2378	27	594	0.249790	0.626156	Occluded
14	Baseline_2_right_wrist_002	2464	27	651	0.264205	0.588068	Occluded
15	Baseline_2_right_wrist_003	2588	27	621	0.239954	0.570325	Occluded
16	Baseline_3_left_knee_002	2680	27	649	0.242164	0.540672	Occluded
17	Baseline_3_left_knee_003	2462	27	681	0.276604	0.578798	Occluded
18	Baseline_3_right_knee_001	2670	27	691	0.258801	0.590262	Occluded
19	Baseline_3_right_knee_002	2450	27	626	0.255510	0.575102	Occluded
20	Baseline_3_right_knee_003	2440	27	679	0.278279	0.610656	Occluded
21	Baseline_variation_003	3164	27	906	0.286346	0.642225	Occluded
22	Baseline_variation_004	1458	27	446	0.305898	0.515775	Occluded

Table 12: Category Summary of Smooth Motion and Motion with Anomalities

Category	Clean motion	Occluded motion	Total
Baseline 1	4	0	4
Baseline 2 (elbows/wrists)	0	11	11
Baseline 3 (knees)	0	5	5
Variations	0	2	2
Total	**4 smooth**	**18 anomalies**	**22 sequences**

Table 13: Occlusion Statistics for the 18 Occluded Sequences

#	Sequence	Frames	Joints	Occluded Frames	Occlusion Rate	Mean Occluded Joints/Frame
1	Baseline_2_left_elbow_002	2696	27	717	0.265950	0.594585
2	Baseline_2_left_elbow_003	2980	27	731	0.245302	0.586577
3	Baseline_2_left_wrist_001	2700	27	681	0.252222	0.626296
4	Baseline_2_left_wrist_003	2578	27	664	0.257564	0.569822
5	Baseline_2_right_elbow_001	2752	27	712	0.258721	0.569767
6	Baseline_2_right_elbow_002	3186	27	847	0.265851	0.655367
7	Baseline_2_right_elbow_003	2482	27	624	0.251410	0.591056

Table 13: Occlusion Statistics for the 18 Occluded Sequences (continued)

#	Sequence	Frames	Joints	Occluded Frames	Occlusion Rate	Mean Occluded Joints/Frame
8	Baseline_2_right_left_elbow_001	2501	27	624	0.249500	0.597361
9	Baseline_2_right_wrist_001	2378	27	594	0.249790	0.626156
10	Baseline_2_right_wrist_002	2464	27	651	0.264205	0.588068
11	Baseline_2_right_wrist_003	2588	27	621	0.239954	0.570325
12	Baseline_3_left_knee_002	2680	27	649	0.242164	0.540672
13	Baseline_3_left_knee_003	2462	27	681	0.276604	0.578798
14	Baseline_3_right_knee_001	2670	27	691	0.258801	0.590262
15	Baseline_3_right_knee_002	2450	27	626	0.255510	0.575102
16	Baseline_3_right_knee_003	2440	27	679	0.278279	0.610656
17	Baseline_variation_003	3164	27	906	0.286346	0.642225
18	Baseline_variation_004	1458	27	446	0.305898	0.515775

On held-out sequences, the detector achieved strong performance across joint types:

Table 14: Implementation and Evaluation Quantitative Results

Joint	Precision	Recall	F1-score
Elbow	0.84	0.80	0.82
Wrist	0.82	0.77	0.79
Knee	0.81	0.79	0.80
Average	**0.82**	**0.79**	**0.80**

Table 15: Summary of Occlusion Presence

Data Tier	Count	Occlusion Found?	Notes
Baseline 1	4	No (0%)	Clean reference sequences
Baseline 2	11	Yes	Elbow/wrist occlusions
Baseline 3	5	Yes	Knee occlusions
Variations	2	Yes	Highest anomaly rates
Total	**22**	**4 clean + 18 occluded**	Final dataset

Using the Z-score detector, the full dataset yielded:

Table 16: Occlusion Statistics Across All 22 Sequences

Dataset Tier	Count	Occlusion Found?	Notes
Baseline 1 (clean)	**4**	No (0%)	Fully visible reference motion
Baseline 2 (upper-limb)	**11**	Yes	Elbow and wrist occlusions
Baseline 3 (lower-limb)	**5**	Yes	Knee occlusions
Variations	**2**	Yes	Highly dynamic, noisy
Total	**22**	**4 clean + 18 occluded**	Final dataset

Table 17: Jerk Reduction After SLERP Reconstruction (18 Occluded Sequences)

Sequence	**Jerk Before**	**Jerk After**	**Improvement** (ΔJ)
Baseline_2_left_elbow_002	0.000067	0.000043	0.000024
Baseline_2_left_elbow_003	0.000037	0.000030	0.000007
Baseline_2_left_wrist_001	0.000044	0.000033	0.000011
Baseline_2_left_wrist_003	0.000057	0.000044	0.000013
Baseline_2_right_elbow_001	0.000073	0.000039	0.000034
Baseline_2_right_elbow_002	0.000038	0.000026	0.000012
Baseline_2_right_elbow_003	0.000051	0.000039	0.000012
Baseline_2_right_left_elbow_001	0.000050	0.000036	0.000014
Baseline_2_right_wrist_001	0.000053	0.000039	0.000014
Baseline_2_right_wrist_002	0.000049	0.000038	0.000011
Baseline_2_right_wrist_003	0.000057	0.000045	0.000012
Baseline_3_left_knee_002	0.000055	0.000041	0.000014
Baseline_3_left_knee_003	0.000080	0.000056	0.000024
Baseline_3_right_knee_001	0.000048	0.000040	0.000008
Baseline_3_right_knee_002	0.000059	0.000047	0.000012
Baseline_3_right_knee_003	0.000056	0.000043	0.000013
Baseline_variation_003	0.000093	0.000074	0.000019
Baseline_variation_004	0.000197	0.000172	0.000025